Protease-Activated Receptor Mediated RhoA Signaling and Cytoskeletal Reorganization in LNCaP Cells†

Daniel L. Greenberg,[‡,§,||] Gregory J. Mize,[‡,§,⊥] and Thomas K. Takayama*[,§,⊥]

Departments of Biochemistry, Medicine, and Urology, University of Washington, Box 357350, Seattle, Washington 98195-7350

Received November 1, 2002; Revised Manuscript Received November 22, 2002

ABSTRACT: Thrombin and trypsin induce cell signaling through a subclass of G-protein-coupled receptors called the protease-activated receptors (PARs). In many cells, PAR signaling results in the activation of RhoA and other members of the Rho family of small GTPases which are involved in cytoskeletal reorganization. The expression of PARs and their role in the activation of Rho GTPases in prostate cancer cells are not clearly known. FACS analysis demonstrated that the androgen-dependent LNCaP cells express PAR1, PAR2, and PAR4 but not PAR3. Stimulation with thrombin and trypsin resulted in the rapid activation of RhoA in a dose-dependent manner with an EC_{50} of 1.0 and 5 nM, respectively. Activation of RhoA was enhanced by, but not dependent on, the presence of 1 nM dihydrotestosterone. Inhibition of the proteolytic properties of thrombin by hirudin and trypsin by diisopropyl fluorophosphate abolished the observed RhoA activation. Stimulation with 150 μM PAR-activating peptides TFFLRN (PAR1), SLIGKV (PAR2), and AYPGKF (PAR4) demonstrated that PAR1 and PAR2 mediated protease-activated RhoA signaling. Fluorescent microscopy studies showed that LNCaP cells treated with either thrombin (10 nM) or trypsin (10 nM) developed an increased number of filopodia, stress fibers, and focal adhesions relative to untreated cells. These observations represent the first report of PAR signaling in prostate cancer cells as well as the ability of PAR2 to mediate RhoA activation. Since the activation of RhoA is important for cytoskeletal reorganization, we postulate that PAR-mediated RhoA activation may be a major signaling pathway in the biology of prostate cancer.

Prostate cancer is the most commonly diagnosed malignancy after skin cancer and the second leading cause of cancer mortality in men in the United States (*1*). As a paracrine gland the prostate primarily functions by secreting a nutrient-rich fluid which comprises about 30% of the total seminal fluid (*2*). Prostatic fluid contains prostate-specific antigen (PSA),[1] a hormonally regulated serine protease that serves as a valuable tumor marker for prostate cancer (*2*). Several prostatic serine proteases, including PSA, are produced by the glandular epithelial cells and secreted into the prostatic fluid. The glandular epithelial cells also express transmembrane serine proteases, including TMPRSS2 (*3*) and hepsin (*4*−*6*). Prostatic serine proteases may cleave specific cellular substrates that influence cell growth and the progression of metastatic prostate cancer (*7*). These cellular substrates have been postulated to include growth factor precursors, regulatory factors of signal transduction and gene transcription, and cell surface protease-activated receptors. In this paper we show that intracellular signaling and cytoskeletal reorganization in the prostate cancer cell line LNCaP can be mediated by the proteolytically active serine proteases, thrombin and trypsin.

A major mechanism by which cellular behavior is influenced by serine proteases is through the activation of the protease-activated receptors (PARs), a subfamily of the G-protein-coupled receptors (GPCRs) (*8*, *9*). PARs are found in a variety of tissues and cells including platelets, endothelial cells, the gastrointestinal tract, the central nervous system, and the lungs. Numerous established cell lines derived from malignant tissues such as breast, colon, lung, and prostate contain mRNA for at least one and usually two or more of the four PARs (*8*). Gene knockout of PAR1 in mice shows normal development in half of the fetuses while the other

† This work was supported in part by Grants DK02447 (T.K.T.) and HL16919 (D.L.G.) from the National Institutes of Health, the Richard M. Lucas Foundation, the American Foundation for Urologic Disease, and the American Cancer Society.

* To whom correspondence should be addressed. E-mail: tomt@u.washington.edu. Fax: (206) 543-5368.

‡ These authors contributed equally.

§ Department of Biochemistry, University of Washington.

|| Department of Medicine, University of Washington.

⊥ Department of Urology, University of Washington.

[1] Abbreviations: PAR, protease-activated receptor; GPCRs, G-protein-coupled receptors; AP, activating peptide; AP-1, TFFLRN (PAR1); AP-2, SLIGKV (PAR2); AP-3, TFRGAP (PAR3); AP-4, AYPGKF (PAR4); FACS, fluorescent-activated cell sorter; GST, glutathione *S*-transferase; RBD, rhotekin binding domain; GST-RBD, glutathione *S*-transferase−RhoA binding domain fusion protein; EC_{50}, effective concentration for 50% response; DFP, diisopropyl flouro-phosphate; DHT, dihydrotestosterone; PSA, prostate-specific antigen; PBS, phosphate-buffered saline; DAPI, 4′,6-diamidino-2-phenylindole; FITC, fluorescein isothiocyanate; HRP, horseradish peroxidase; ECL, enhanced chemiluminescence; FBS, fetal bovine serum; GSH, glutathione; SDS−PAGE, sodium dodecyl sulfate−polyacrylamide gel electrophoresis; TBS, Tris-buffered saline; AR, androgen receptor; GEF, guanine exchange factor; RGS, regulation of G-protein signaling; RT-PCR, reverse transcription polymerase chain reaction; RXR, retinoic acid receptor; PIP5 kinase, phosphatidylinositol 4-phosphate 5-kinase.

10.1021/bi027100x CCC: $25.00
Published on Web 12/31/2002

half die at embryonic day 9, possibly from the abnormal development of the vasculature (*8*). PAR2, PAR3, and PAR4 gene knockouts in mice develop normally, suggesting functional redundancies or cross-talk among this family of receptors (*8*, *10*).

Proteolytic cleavage of the amino-terminal extracellular domain of the PARs exposes new amino termini which act as a "tethered ligand" to cause receptor activation (*8*). The newly exposed tethered ligand binds intramolecularly to the second extracellular loop of the receptor to induce signal transduction. Three of the four PARs (PAR1, PAR3, and PAR4) are activated by thrombin while PAR2 is activated by trypsin-type serine proteases (*8*, *9*). PAR4 is unique in that it is activated by either thrombin or trypsin (*8*, *9*); however, the physiologic role of the trypsin activation of PAR4 is unknown. PAR1, PAR2, and PAR4 can be selectively activated by micromolar concentrations of the specific hexapeptides corresponding to the exposed tethered ligand. Accordingly, TFFLRN (AP-1) activates PAR1, SLIGKV (AP-2) activates PAR2, and AYPGKF (AP-4) activates PAR4 (*8*, *9*).

PAR intracellular signaling leading to Rho activation appears to involve two major signal transduction pathways: the $G_{\alpha q}$-coupled system resulting in phosphoinositol hydrolysis and calcium-dependent Rho activation or the calcium-independent direct activation of Rho through $G_{\alpha 12/13}$-coupled p115Rho-GEF (*11*). PAR signaling through the activation of the Rho family proteins is important because they have been shown to mediate vital cellular functions including regulation of the cytoskeleton (*11*). Rho family proteins are members of a major branch of the Ras superfamily of small GTPases and share approximately 30% amino acid identity with Ras. Like Ras and the Gα subunits of heterotrimeric G-proteins, Rho family proteins function as GTP/GDP regulated switches that cycle between active GTP-bound and inactive GDP-bound forms. The activated, or GTP-bound, Rho GTPases are able to interact with a broad spectrum of diverse effectors to carry out their cellular functions. Of the 14 mammalian members of the Rho family GTPases, RhoA is the most well characterized. RhoA plays a central role in regulating the formation of actin stress fibers and focal adhesions as a result of extracellular stimuli (*11*). Constitutively activated RhoA increases the invasive properties and metastatic potential of many tumor cells (*11*). RhoA-regulated Rho kinase is directly involved in the regulation of myosin light chain phosphorylation and the formation of cytoskeletal actin−myosin filaments (*11*). These cytoskeletal changes are essential components for cancer cell growth and metastasis since invasion through vessel walls as well as cell division requires extensive cytoskeletal reorganizations, which are regulated, in part, by the Rho GTPases.

Sensitive assays to directly demonstrate RhoA activity in response to extracellular stimuli have recently been developed. To demonstrate PAR signaling in LNCaP cells, we have employed the RhoA "trapping assay" in which GTP-bound RhoA from cell lysates is "trapped" by a GST fusion protein containing the RhoA binding domain of the mouse protein rhotekin (*12*). While the physiologic function of rhotekin is unknown, it avidly binds RhoA-GTP but does not bind RhoA-GDP or RhoA (*13*).

Little is known regarding PAR expression and PAR-signaling pathways in prostate cancer cells, although prostate tissue synthesizes several serine proteases that may be potential PAR activators. PC-3 cells exposed to thrombin show an increased production of urokinase, a serine protease that has been implicated in cancer cell invasion (*14*). No studies have been reported investigating cellular responses to serine proteases in the testosterone-dependent prostate cell line, LNCaP.

In this report we show that three of the four known PARs, PAR1, PAR2, and PAR4, are expressed by LNCaP cells. Low concentrations of either trypsin or thrombin cause RhoA activation in LNCaP cells. The activation of cytosolic RhoA is dependent on the proteolytic activities of these extracellular proteases and enhanced by dihydrotestosterone (DHT). Selective PAR activation with hexapeptides shows that PAR1 and PAR2 are the primary mediators of RhoA activation. Along with RhoA activation, thrombin and trypsin also cause cytoskeletal rearrangement and the formation of stress fibers and focal adhesions in LNCaP cells. This represents the first observation of RhoA signaling and cytoskeletal rearrangement in prostate cancer cells and is most likely the result of direct PAR1 and PAR2 activation by the serine proteases thrombin and trypsin.

EXPERIMENTAL PROCEDURES

Materials. Human α-thrombin (specific activity 3147 NIH units/mg; 7838 NIH units/mL) was purchased from Enzyme Research Labs (South Bend, IN). Trypsin was kindly provided by Dr. Kazuo Fujikawa (Department of Biochemistry, University of Washington, Seattle, WA). Miscellaneous chemicals, saponin, phosphate-buffered saline (PBS), DNase I, protease inhibitor cocktail, paraformaldehyde, diisopropyl flourophosphate (DFP), dihydrotestosterone (DHT), 4′,6-diamino-2-phenylindole (DAPI), fluorescein isothiocyonate (FITC) conjugated rabbit anti-goat antibodies, and hirudin were purchased from Sigma Chemical Co. (St. Louis, MO). Texas Red-X phalloidin was purchased from Molecular Probes (Eugene, OR). Rabbit anti-androgen receptor antibodies, goat and rabbit anti-PAR antibodies, FITC-conjugated goat anti-rabbit IgG, and horseradish peroxidase (HRP) conjugated anti-RhoA antibodies were purchased from Santa Cruz Biotechnology (Santa Cruz, CA). GSH Sepharose beads and the ECL Plus Western blot detection kit were purchased from Amersham Biosciences (Piscataway, NJ). Amidated PAR-activating peptides were purchased from Anaspec (San Jose, CA).

Cell Culture. LNCaP cells obtained from the ATCC (Manassas, VA) were cultured in RPMI 1640 supplemented with 10% fetal bovine serum (FBS) or 10% charcoal-stripped FBS from Gemini Bio-products (Woodland, CA). Penicillin (100 units/mL) and streptomycin (100 μg/mL) from Gibco Invitrogen (Grand Island, NY) were also added to the culture media, and the cells were grown under 5% CO_2 at 37 °C. DHT (1 nM) was added to the cells once they were shifted into charcoal-stripped FBS.

Flow Cytometry. LNCaP cells grown to 80% confluence on 10 cm plates were washed twice with PBS (10 mM sodium phosphate, pH 7.4, 120 mM NaCl, 2.7 mM KCl) and detached from the plates with 0.5 mM EDTA in PBS. The detached cells were then suspended in PBS containing 1 mM EDTA and 2% FBS. After two washes in PBS, the cells were suspended in PBS containing 0.3% saponin and

aliquoted into microcentrifuge tubes. The primary antibodies (either anti-PAR or anti-androgen receptor) were added to a final dilution of 1:100 from the commercially supplied stock solution. The primary antibodies were incubated with the cells for 90 min at 4 °C with gentle mixing. The cells were then washed twice with PBS containing 0.1% saponin to remove unbound primary antibodies. The cells were then suspended in PBS containing 0.3% saponin, and secondary antibodies (FITC-conjugated rabbit anti-goat or FITC-conjugated goat anti-rabbit IgG) were added to a final antibody dilution of 1:400 of the commercially supplied stock solution and incubated for 90 min at 4 °C with gentle mixing. The cells were again washed twice with PBS containing 0.1% saponin to remove unbound secondary antibodies. Finally, the cells were suspended and fixed in PBS containing 0.5% paraformaldehyde. The antibody-labeled samples were then analyzed on a Becton Dickinson FACScan (San Jose, CA) flow cytometer.

Rhotekin Trap Assay. Originally described by Ried et al., this assay was developed to measure the activation of RhoA in cultured cells (*12*). A 266 bp (81 amino acid) open reading frame of rhotekin cDNA containing the RhoA binding domain (*13*) was amplified by PCR from a mouse brain cDNA library (courtesy of Dr. Weng-Feng Xu, Zymogenetics, Seattle, WA). The amplified fragment was ligated into the vector pGEX-6XP-1 (Stratagene, La Jolla, CA) using *Hin*dIII and *Kpn*I linkers. The resulting construct, pGEX-RBD, expresses a chimeric protein containing glutathione *S*-transferase (GST) fused to the 81 amino acid RhoA binding domain (RBD) of rhotekin. After verification of the sequence by DNA sequencing, the fusion protein (GST-RBD) was expressed in *Escherichia coli* BL21 cells (Invitrogen, Carlsbad, CA) by induction with isopropyl thiogalactoside (IPTG) and isolated from the cell lysate by binding to glutathione (GSH)−Sepharose 4B. The fusion protein bound to the GSH beads was stored at −70 °C in a buffer containing 10% glycerol.

Once the GST-RBD fusion protein was isolated, the concentration was assessed by SDS−PAGE and compared to known amounts of bovine serum albumin. To determine the ability of the GST-RBD to bind RhoA-GTP and to standardize the binding activities in different GST-RBD preparations, serum starved NIH 3T3 cells (ATCC, Manassas, VA) were stimulated with media containing 10% fetal calf serum for 3 min, and the assay was completed as described below. Under these conditions, lysophosphatidic acid present in serum typically converts 3% of the total RhoA to the RhoA-GTP form (*15*). The amount of GST-RBD necessary to adsorb all of the RhoA-GTP is about 15−20 μg.

After each new preparation of GST-RBD was tested and standardized with NIH-3T3 cells, experiments were performed on LNCaP cells. The LNCaP cells were grown to 80% confluence on 10 cm plates as described. The cells were then washed and cultured in media supplemented with 10% charcoal-stripped FBS and 1 nM DHT. After 24 h, the cells were washed thoroughly. Stimulation of the PARs with thrombin or trypsin was then performed in 5 mL of serum-free RPMI 1640. For dose-dependent responses, the cells were treated with the protease activators at various concentrations for 3 min. To determine the temporal response of RhoA charging, the cells were stimulated with an appropriate dose of each protease for the time intervals shown. Stimulated cells were washed twice after stimulation with TBS (25 mM Tris-HCl, pH 7.5, 137 mM NaCl, 5 mM KCl, 0.5 mM $MgCl_2$, 0.37 mM Na_2HPO_4, 0.9 mM $CaCl_2$) and lysed with RIPA buffer (50 mM Tris-HCl, pH 7.2, 1% Triton X-100, 0.1% SDS, 500 mM NaCl, 10 mM $MgCl_2$) supplemented with 30 nM DNase I and protease inhibitor cocktail (18 mM AEBSF, 8 μM aprotinin, 0.36 mM bestatin, 0.15 mM pepstatin A, 0.14 mM E-64, and 0.21 mM leupeptin). The lysed cells were immediately placed on ice, and all subsequent steps were performed at 4 °C. Cell lysates were clarified by centrifugation (13000g for 3 min) and incubated with the GST-RBD fusion protein for 1 h with gentle rocking. The conjugated beads were then washed with 50 mM Tris-HCl, pH 7.5, 1% Triton X-100, 10 mM $MgCl_2$, and 150 mM NaCl, resuspended in SDS−PAGE loading buffer, and analyzed by Western blot using HRP-conjugated anti-RhoA antibodies. For comparison, a small amount of total cell lysate corresponding to each condition of stimulation was also blotted alongside the GST-RBD pull-down material. Western blot detection was done with the ECL Plus detection kit and exposed on Kodak (Rochester, NY) X-Omat Blue XB-1 film.

DAPI/Phalloidin Staining. LNCaP cells were grown on plastic chamber slides (Nalgene Nunc International, Naperville, IL) to subconfluence. The cells were washed with PBS for 5 min, fixed with 2% paraformaldehyde for 30 min, and washed again with PBS at room temperature. In the dark, cells were stained with a solution of 11 μM DAPI and 66 nM Texas Red-X phalloidin in PBS containing 1% BSA and 0.05% Triton X-100 for 30 min at room temperature. After being stained, the cells were washed three times with PBS. A drop of mounting media (Vectashield, Vector Labs, Burlingame, CA) was added to the slide followed by a cover slip. The slides were visualized on a Nikon (Garden City, NJ) Eclipse E800 fluorescent microscope and analyzed with MetaMorph 4.1 software (Universal Imaging Corp., Downington, PA).

RESULTS

FACS Analysis of PARs in LNCaP Cells. To determine the presence of PARs on LNCaP cells, flow cytometry was performed using PAR-specific antibodies. For comparison, these cells were also analyzed for the presence of androgen receptor (AR). Fluorescence shifts are present with antibodies directed against three of the PARs and AR (Figure 1). The minimal shift observed with anti-PAR3 antibodies was not affected by a specific anti-PAR3 blocking peptide (data not shown). The shifts seen with anti-PAR1, PAR2, PAR4, and AR antibodies were substantially reduced by similar antibody blocking peptides, demonstrating that the shift seen with the anti-PAR3 antibodies represents nonspecific binding (data not shown). PAR2 appears to be moderately abundant while PAR1, PAR4, and AR are highly abundant. These data are comparable to FACS analysis of PARs with breast cancer cells, in which PAR1, PAR2, and PAR4 are expressed but PAR3 is absent (*16*). The results shown here are representative of at least four experiments with anti-PAR and anti-AR antibodies.

RhoA Activation Is Mediated by Extracellular Thrombin and Trypsin. LNCaP cells were incubated with thrombin (10

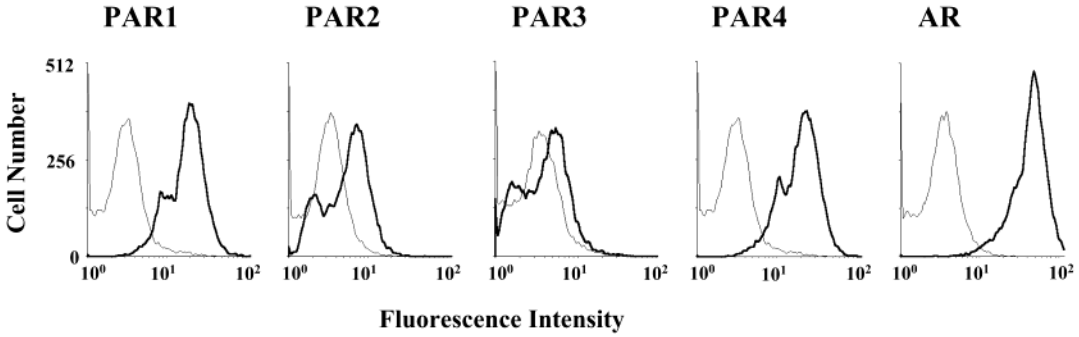

FIGURE 1: PAR expression profile of LNCaP cells. Cells were stained as described in the Experimental Procedures. FITC-labeled cells were analyzed by flow cytometry. Key: light tracing, background fluorescence (secondary antibody alone); dark tracing, fluorescence shift attributable to PAR expression. For comparison, androgen receptor expression is shown in the last panel. Fluorescence shifts attributable to PAR1, PAR2, and AR, but not PAR3, were abolished by antibody blocking peptides (see text). Traces shown are representative of four independent experiments.

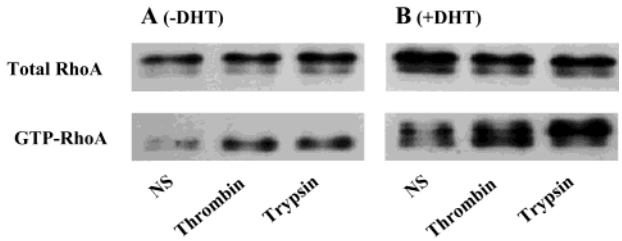

FIGURE 2: RhoA activation by thrombin and trypsin. Rhotekin trap assays from LNCaP cell lysates after 3 min exposure to buffer (NS), thrombin (10 nM), or trypsin (10 nM). Panel A: Cells were shifted to growth media containing charcoal-stripped FBS. Panel B: The same growth media supplemented with 1 nM DHT. These Western blots are representative of three independent experiments.

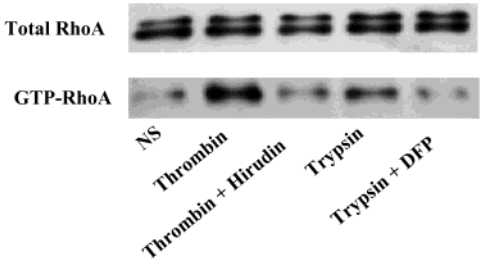

FIGURE 3: Dependence of RhoA activation on proteolysis by trypsin or thrombin. Rhotekin trap assay from LNCaP cell lysates after 3 min exposure to buffer (NS), thrombin (10 nM), thrombin inhibited with hirudin (50 nM), trypsin (10 nM), or trypsin inhibited with DFP (10-fold molar excess). Inactivation of trypsin by DFP and thrombin by hirudin was verified by incubation with their respective chromogenic substrates, S-2222 and S-2238 (data not shown). These blots are comparable with the results from three separate experiments.

nM) and trypsin (10 nM) to determine if they signal through RhoA in response to extracellular proteolysis of the PARs. The rhotekin trap assay (as described in the Experimental Procedures) was used to analyze RhoA activation.

LNCaP cells grown in media containing 10% FBS were shifted to media containing 10% charcoal-stripped (steroid hormone depleted) FBS. The cells were incubated with or without 1 nM dihydrotestosterone (DHT) for 24 h. LNCaP cells were then activated for 3 min in serum-free media with thrombin (10 nM), trypsin (10 nM), or buffer alone. Results show that both thrombin and trypsin stimulations increase the activated (GTP-bound) RhoA in the LNCaP cells (Figure 2). Stimulation with either thrombin or trypsin results in comparable amounts of RhoA activation. Comparison of panels A and B in Figure 2 demonstrates that, for the same stimulatory conditions, LNCaP cells treated with DHT have increased total RhoA (upper row) and proportionately increased activated (GTP-bound) RhoA (lower row) relative to cells treated without DHT. Similar experiments with different concentrations of DHT for various incubation times showed that optimal RhoA activation was observed with 1 nM DHT for 24 h (data not shown). The subsequent experiments described in this report were performed after the cells were incubated for 24 h with steroid hormone depleted (charcoal-stripped) FBS supplemented with 1 nM DHT.

Extracellular Thrombin or Trypsin Must Be Proteolytically Active To Cause Intracellular RhoA Activation. LNCaP cells were incubated with inactivated proteases to determine if intracellular RhoA activation is dependent on the proteolytic activities of trypsin or thrombin. Thrombin inactivation was carried out with a 5-fold molar excess of hirudin, a thrombin-specific inhibitor, and trypsin was inactivated with a 10-fold molar excess of diisopropyl fluorophosphate (DFP), a potent serine protease inhibitor (*17*, *18*). Both inhibited enzymes had no residual amidolytic activity when measured by cleavage of their respective chromogenic substrates, S-2222 (trypsin) and S-2238 (thrombin; data not shown). Compared with the substantial amount of activated RhoA with 10 nM thrombin (Figure 3, lane 2), hirudin-inhibited thrombin (Figure 3, lane 3) resulted in no measurable increase in RhoA activation beyond that observed in the buffer control. Similar results occurred with 10 nM trypsin (Figure 3, lane 4) and trypsin inhibited with DFP (Figure 3, lane 5). These observations are consistent with published studies showing that RhoA-GTP formation is mediated by proteolytic activation of PARs (*15*).

Low Concentrations of Thrombin Mediate the Rapid Activation of Intracellular RhoA. To determine the dependence of intracellular RhoA activation on thrombin concentration, LNCaP cells were activated with thrombin at concentrations ranging from 0.1 to 25 nM. RhoA activation is detectable even at 0.1 nM thrombin (Figure 4A, lane 2). Half-maximum RhoA activation occurred at 0.5−1.0 nM, and maximal RhoA activation occurred at 2.5 nM thrombin. At thrombin concentrations from 5 to 25 nM, RhoA activation reaches a plateau. The activation of RhoA at low (<1 nM) thrombin suggests that LNCaP cells are very sensitive to thrombin. Activation of RhoA in platelets occurs

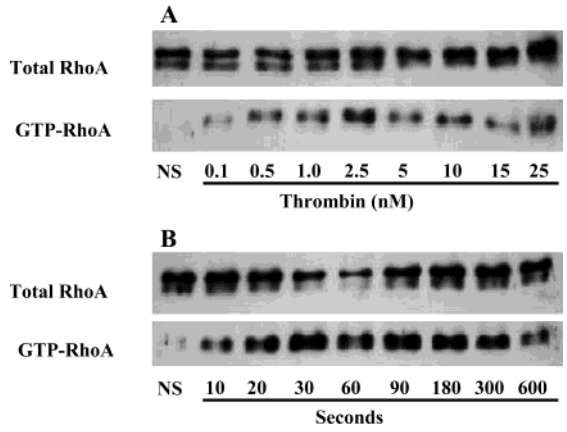

FIGURE 4: RhoA activation by thrombin is dose dependent and occurs rapidly. Panel A: Rhotekin trap assay from LNCaP cell lysates after cells were incubated for 3 min with thrombin concentrations ranging from 0.1 to 25 nM. Panel B: Rhotekin trap assay from LNCaP cell lysates after cells were incubated for the indicated time with 10 nM thrombin. These results are representative of two independent experiments.

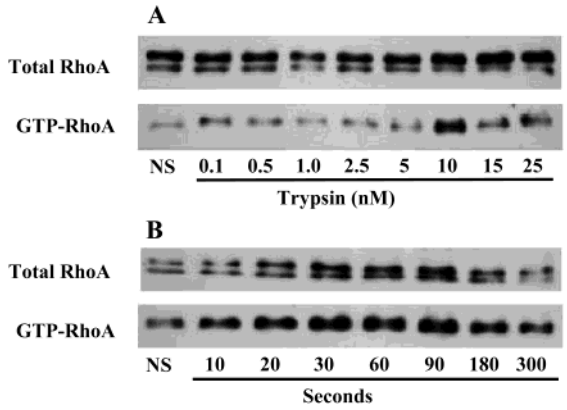

FIGURE 5: RhoA activation by trypsin occurs at a threshold concentration and occurs rapidly. Panel A: Rhotekin trap assay from LNCaP cell lysates after cells were incubated for 3 min with trypsin concentrations ranging from 0.1 to 25 nM. Panel B: Rhotekin trap assay from LNCaP cell lysates after cells were incubated for the indicated time with 10 nM trypsin. These results are representative of two independent experiments.

at thrombin concentrations of 1−4 nM (*19*, *20*), which is consistent with the results shown here of maximum RhoA activation induced by 2.5 nM thrombin.

To determine the rate of RhoA activation by thrombin, LNCaP cells stimulated with 10 nM thrombin were lysed at different time points and analyzed for RhoA activation (Figure 4B). Substantial RhoA activation is observed within 10 s and maximal RhoA activation within 30 s. RhoA activation plateaus at the maximum from 30 to 300 s. Rapid RhoA activation by thrombin in LNCaP cells was comparable to those observed within platelets and NIH3T3 cells (*15*).

The Activation of RhoA Is Stimulated by a Threshold Concentration of Trypsin and Occurs Rapidly. To characterize the dependence of trypsin concentration on the activation of intracellular RhoA, LNCaP cells were incubated with trypsin at concentrations ranging from 0.1 to 25 nM. RhoA activation by trypsin is minimal up to 10 nM (Figure 5A). Maximum activation of RhoA occurs with 10 nM (Figure 5A) and does not increase with higher concentrations. These

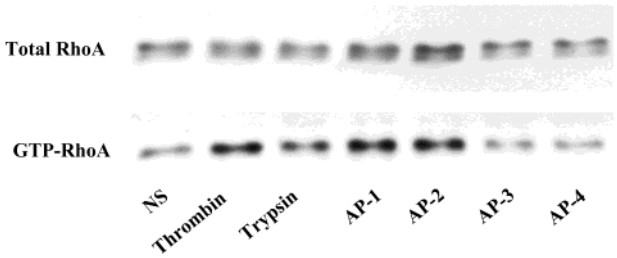

FIGURE 6: RhoA activation is mediated by PAR1 and PAR2. Rhotekin trap assay from LNCaP cell lysates after 3 min exposure to buffer (NS), thrombin (10 nM), trypsin (10 nM), and 150 μM AP-1 (TFFLRN), AP-2 (SLIGKV), AP-3 (TFRGAP), or AP-4 (AYPGKF). Stimulation of LNCaP cells with thrombin or trypsin shows a similar amount of RhoA activation as AP-1 and AP2. Stimulation with AP-3 and AP-4 shows no increase in RhoA activation relative to nonstimulatory control. These results are representative of four independent experiments.

results show that the threshold for optimal RhoA activation by trypsin occurs at 10 nM.

The time-dependent activation of RhoA (Figure 5B) shows that trypsin-induced activation of RhoA is also rapid, occurring within 10 s. The maximum RhoA activation by 10 nM trypsin is observed within 30 s and plateaus at the maximum from 60 to 300 s. Taken together, these data show that a threshold concentration of 10 nM trypsin results in the rapid and sustained activation of RhoA in LNCaP cells.

PAR1 and PAR2 Are the Primary Mediators of RhoA Activation. PAR-activating peptides were used to determine which of the individual PARs mediates RhoA activation in LNCaP cells. The activation of RhoA by 150 μM TFFLRN (AP-1), SLIGKV (AP-2), and AYPGKF (AP-4) was analyzed (Figure 6). TFRGAP (AP-3) corresponds to the tethered ligand exposed by PAR3 activation by thrombin and is used as a negative peptide control since PAR3 cannot be activated by this hexapeptide (*8*). The amount of RhoA-GTP in response to AP-1 and AP-2 is comparable with 10 nM thrombin or 10 nM trypsin, respectively. Stimulation with AP-3 and AP-4 and buffer alone (NS) shows baseline RhoA activation. These data indicate that PAR1 and PAR2 are responsible for PAR-mediated RhoA activation in LNCaP cells.

LNCaP Cells Stimulated with Thrombin and Trypsin Show Cytoskeletal Reorganization. DAPI/Texas Red-X phalloidin staining of LNCaP cells was performed to determine if the biochemical activation of RhoA by thrombin and trypsin results in cytoskeletal reorganization. In these experiments, LNCaP cells were grown to 75% confluence on four-well chamber slides. The cells were incubated in media containing charcoal-stripped FBS supplemented with 1 nM DHT for 24 h and then stimulated with 10 nM thrombin, 10 nM trypsin, or buffer alone in serum-free media (with DHT) for 48 h.

Resting LNCaP cells show typical epithelial cell morphologic features of slightly elongated, stellate shape with perinuclear central roundness (Figure 7A). Texas Red-X phalloidin stained actin concentrates around the DAPI-stained blue nuclei (labeled N with arrows, Figure 7) and evenly distributes throughout the cytoplasm. After about 8 h, cells treated with 10 nM thrombin or 10 nM trypsin begin to show cytoskeletal reorganization. After 48 h, the cells project fingerlike filapodia (labeled F, Figure 7B) containing actin filaments. Cells also develop punctate focal adhesions

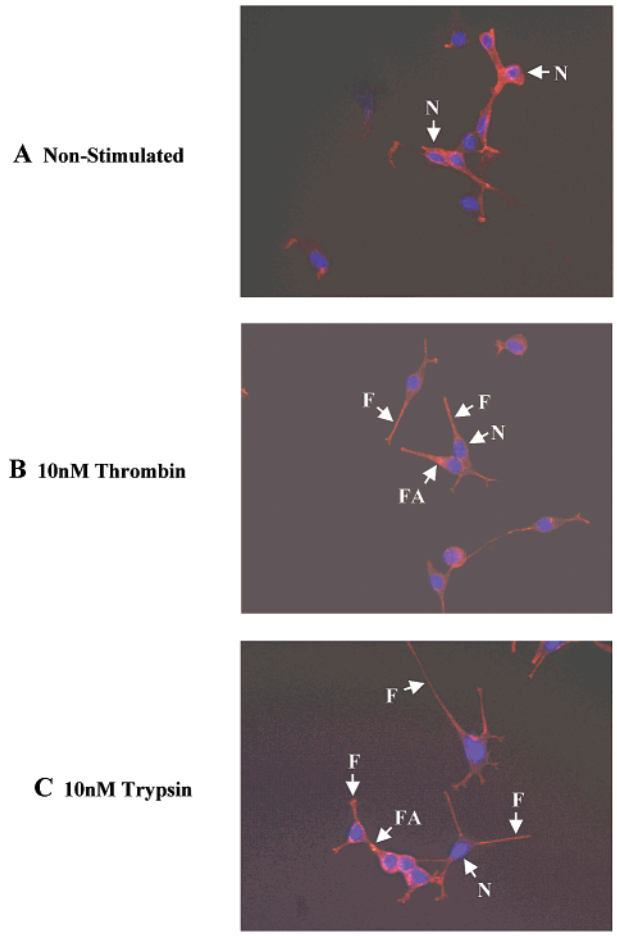

FIGURE 7: Cytoskeletal reorganization of LNCaP cells by trypsin and thrombin. DAPI/phalloidin staining was performed as described in the Experimental Procedures. Key: N, nuclear staining by DAPI; F, filapodia formation; FA, focal adhesions as demonstrated by actin staining with phalloidin.

connected with stress fibers consisting of thick actin bundles (labeled FA, Figure 7B). Similar fingerlike projections and focal adhesions with connecting stress fibers (Figure 7C) are shown to result from treatment with 10 nM trypsin. These results demonstrate that cellular shape changes and focal adhesions are induced by stimulation of LNCaP cells with either thrombin or trypsin.

DISCUSSION

The results of this study show that functional PAR1, PAR2, and PAR4 are expressed on LNCaP cells. The potential role of PAR1-mediated cytoskeletal reorganization in the LNCaP cells may be illustrated by the mechanisms involved in platelet shape change. As in platelets, the expression of PAR1 on LNCaP cells seems to account for the activation of RhoA by thrombin. The EC_{50} of thrombin for PAR1 has been reported as 0.5 nM in transfected cell lines (*21*) as well as in platelets (*8*). The results of maximum RhoA activation at thrombin concentrations of 2.5 nM and above together with comparable RhoA activation by AP-1 suggests that PAR1 plays a major role with respect to RhoA signaling in LNCaP cells. The ability of PAR1 to signal through RhoA is well established. In human platelets, which undergo extensive spreading and shape change when exposed to thrombin (*22*), PAR1 has been shown to activate RhoA through p115Rho-GEF, a GTP exchange factor (GEF) that associates with the PAR1-coupled G-proteins, $G_{\alpha 12/13}$ (*23*). Activated RhoA then stimulates Rho kinase to phosphorylate myosin light chain kinase and myosin light chain phosphatase, resulting in the formation of myosin filaments and cellular shape changes (*24*).

In prostate cancer cells, cellular shape change is associated with tumor invasion and growth. In particular, actin−myosin reorganization is necessary for tumor invasion through the endothelial cell barrier, and microtubule formation is required for cell division. Consequently, RhoA activation is likely involved in prostate cancer invasion and cellular growth. Inhibition of Rho kinase in PC-3 cells results in a significant decrease in their metastatic potential and invasiveness (*25*). However, there are no published reports describing Rho family GTPase signaling in prostate cancer cell lines. Thrombin-mediated PAR1 responses that have been shown to be a result of RhoA or Rho kinase activation include growth transformation and stress fiber formation in NIH3T3 fibroblasts (*11*), activation of cell rounding and apoptosis in cultured neurons and astrocytes (*26*, *27*), stimulation of smooth muscle migration and DNA synthesis, and endothelial cell contraction and cell barrier dysfunction (*28*, *29*).

Although increased PAR1 levels can mediate growth transformation in NIH3T3 cells as described above, there are variable reports regarding the role of PAR1 in cancer processes. Recently, Even-Ram and co-workers demonstrated that PAR1 expression levels directly correlated with the degree of invasiveness in both primary breast tissue specimens and established cancer cell lines (*30*). High levels of PAR1 mRNA were found in infiltrating ductal carcinoma in contrast to very low amounts in normal and premalignant atypical ductal hyperplasia. Transfection of the invasive breast cancer cells with antisense PAR1 mRNA abolished thrombin-stimulated tumor cell invasion. In another study, a highly metastatic breast cancer cell line was found to express high levels of PAR1, PAR2, and PAR4 while a noninvasive, low metastatic breast cancer cell line expressed low levels of PAR2 and PAR4 and trace levels of PAR1 (*16*). Intracellular calcium signaling was also much greater in the highly metastatic cell line when the PARs were activated by thrombin or PAR-activating peptides. Surprisingly, thrombin signaling through PAR1 inhibited cell invasion in the highly metastatic breast cancer cell line while PAR2 and PAR4 acted as chemokine receptors in both the invasive and minimally invasive cell lines. These findings suggest that there is a complex interplay of PAR-signaling pathways underlying the cellular responses to PAR activation.

There are clearly differences between thrombin- and trypsin-mediated activation of PARs in the LNCaP cells. In contrast to the RhoA activation mediated by increasing concentrations of thrombin up to a maximum plateau at 2.5 nM in LNCaP cells, activation by trypsin occurs at a threshold concentration of 10 nM and then declines. In transfected cell systems the EC_{50} of trypsin for PAR2 activation has been reported as 1 nM, and for PAR4 the EC_{50} of trypsin is 5 nM (*21*, *31*). At 10 nM trypsin, one would expect all of the PAR2 and most of the PAR4 to be activated. Since AP-2 alone is able to activate RhoA comparably to trypsin and AP-4 does not cause RhoA activation in LNCaP cells, it is likely that the RhoA response to trypsin is mediated by PAR2 and not by PAR4. Even though PAR4 does not

mediate RhoA activation in LNCaP cells, PAR4 may still be involved in cytoskeletal reorganization through the activation of other small GTPases.

While several laboratories have demonstrated PAR1 signaling, there are far fewer studies concerning PAR2 and PAR4 signaling. Like PAR1, the cellular responses to PAR2 stimulation depend on the cell type. PAR2 activation has been found to inhibit cellular differentiation and proliferation in epidermal keratinocytes (*32*). This effect may be due to the PAR2-mediated cytokine production and release by keratinocytes rather than directly through PAR2 intracellular signaling. In other cell lines, PAR2 has a stimulatory effect on growth and migration. For example, PAR2 has been shown to increase mitogenesis of vascular smooth muscle cells, increase adhesion and migration of leukocytes, and increase proliferation in pancreatic epithelial cells (*8*, *9*). There are no published studies describing PAR2 signaling through RhoA activation.

An interesting observation shown in this report is the enhancement of the RhoA signaling by DHT because this finding may be a reflection of a novel androgen-dependent RhoA signaling pathway. LNCaP cells are distinguished from other prostate tumor cell lines in that their growth is dependent on the presence of testosterone. PC-3 and DU145 cells, the two other commonly used prostate tumor cell lines, are not dependent on testosterone for growth, although they do express androgen receptor. The enhancement of RhoA activation in the presence of hormone suggests a regulatory effect of the androgen receptor with respect to RhoA signaling. Rubino et al. found an estrogen-regulated RhoA family GTPase-activating protein (GEF) by probing a breast cancer cell expression library for proteins that interacted with the retinoic acid receptor (RXR) (*33*). The cDNA that corresponded to the protein which bound to RXR was named Brx for breast cancer nuclear receptor-binding auxiliary protein. The Brx cDNA predicted a 1428 amino acid protein that contains an estrogen receptor binding domain and a DH-PH domain, which is common to almost all GEFs. The Brx DH-PH domain shares 95% amino acid sequence identity with the DH-PH domain of Lbc. Lbc is a truncated GEF that is oncogenic and is associated with the acute blast crisis of chronic myelogenous leukemia (*34*). The proto-oncogene corresponding to Lbc may be Brx, given the considerable amino acid sequence identity between the overlapping DH-PH domains of these proteins. Unlike Lbc, which activates the RhoA, Brx appears to activate CDC42. CDC42 is a Rho family GTPase that is associated with the formation of filapodia in many cell types and plays an important role in other cell functions such as membrane trafficking (*35*, *36*). The characterization of Brx as a GEF regulated by estrogen receptor further supports the hypothesis that there may be an androgen receptor regulated GEF in prostate cells. In this study, the enhancement of RhoA activation by thrombin and trypsin in LNCaP cells is minimal until 24 h of treatment with 1 nM DHT (data not shown), suggesting that testosterone is influencing the gene regulation of specific factors which are important in RhoA signal transduction. Further studies of Rho family GTPase activation with androgen receptor blockade, inhibition of cellular protein synthesis, and phosphorylation will be necessary to characterize the effects of androgen receptor on Rho signaling.

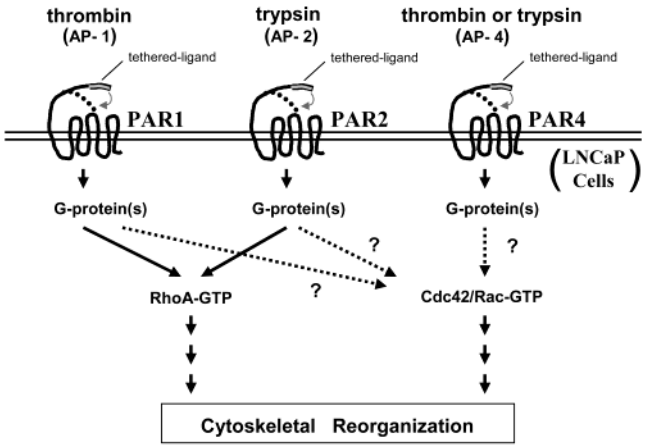

FIGURE 8: Schematic diagram showing PAR1 and PAR2 activation of RhoA in LNCaP cells. PAR4 does not signal through RhoA in these cells but may be involved in other G-protein-coupled signaling pathways leading to the activation of CDC42 or Rac (dotted arrows). PAR1 and PAR2 probably activate more than one heterotrimeric G-protein complex, resulting in the activation of one or more Rho-GEFs. PAR1 and PAR2 may also activate CDC42 and Rac (dotted arrows). Downstream effectors of activated RhoA (RhoA-GTP) lead to cytoskeletal reorganization and other cellular events.

The thrombin- or trypsin-mediated filapodia formation in the LNCaP cells may be a result of a complex mechanism of cytoskeletal reorganization regulated by the Rho family of small GTPases. It is possible that, like human platelets, PAR activation in the LNCaP results in generating activated RhoA, subsequent increased activity of Rho kinases, and eventual change in the activities of myosin light chain kinase and/or phosphatase. The ultimate result is the formation of focal adhesions created by actin and myosin reorganization. Alternatively, PAR activation may generate the activated forms of the other two major Rho family GTPases, Rac and CDC42. Increased levels of the activated Rac may result in the activation of phosphatidylinositol 4-phosphate 5-kinase (PIP5 kinase) and the ARP2/3 complex, which then participate in the organization of filamentous actin to form lamellopodia (*37*). In contrast, increased levels of activated CDC42 may generate p21-activated kinase (*38*) which ultimately leads to the formation of filopodia. It is likely that future studies with various trapping assays for the different Rho GTPases (RhoA, Rac, and CDC42) will elucidate the specific pathway(s) involved in cytoskeletal reorganization in these cells. Furthermore, it is possible that more than one GEF may be involved in the activation of these GTPases. Alternatively, there may be cell-specific differences in the interaction between the various GEF's and the GTPases that regulate specific cytoskeletal changes.

The presence of PARs on LNCaP cells and the activation of RhoA by trypsin, thrombin, or the PAR-activating peptides AP-1 and AP-2 are all consistent with PAR1- and PAR2-mediated signaling. The potential signaling pathways involved in cytoskeletal reorganization mediated by PARs in the LNCaP cells are illustrated (Figure 8). In particular, thrombin may activate either PAR1 to generate active RhoA and CDC42/Rac or also activate PAR4 to generate only active CDC42/Rac. On the other hand, trypsin may mediate its effect on cytoskeletal reorganization through PAR2 and/or PAR4, which results in the increase of their corresponding GTPase(s). These results have particular significance given

the evidence that overexpression of PAR1, and possibly PAR2, results in RhoA-dependent oncogenic transformation and is associated with tumor invasion and metastasis. If prostate cancer progression is in part due to Rho-mediated cytoskeletal reorganization, then the Rho family GTPases may be potentially important targets for small molecule inhibitors. Use of such inhibitors could form the basis of novel therapeutic strategies for the treatment of prostate cancer.

ACKNOWLEDGMENT

The authors acknowledge the following individuals at the University of Washington: Dr. Dominic W. Chung and Dr. Kazuo Fujikawa for many helpful discussions and careful review of the manuscript, Brad A. McMullen for technical assistance, Dr. Paul H. Lange and Dr. Robert Vessella for support and encouragement, Dr. Themis R. Kyriakides for help with DAPI/phalloidin experiments, and Dr. Dennis M. Willerford for help with FACS data.

REFERENCES

1. Jemal, A., Thomas, A., Murray, T., and Thun, M. (2002) *Ca—Cancer J. Clin. 52*, 23−47.
2. Ward, A., Catto, J., and Hamdy, F. (2001) *Ann. Clin. Biochem. 38*, 633−651.
3. Lin, B., Ferguson, C., White, J. T., Wang, S., Vessella, R., True, L. D., Hood, L., and Nelson, P. S. (1999) *Ca Res. 59*, 4180−4184.
4. Dhanasekaran, S., Barrette, T., Ghosh, D., Shah, R., Varambally, S., Kurachi, K., Pienta, K., Rubin, M., and Chinnalyan, A. (2001) *Nature 412*, 822−826.
5. Luo, J., Duggan, D. J., Chen, Y., Sauvageot, J., Ewing, C. M., Bittner, M. L., Trent, J. M., and Isaacs, W. B. (2001) *Cancer Res. 61*, 4683−4688.
6. Magee, J. A., Araki, T., Patil, S., Ehrig, T., True, L., Humphrey, P. A., Catalona, W. J., Watson, M. A., and Milbrandt, J. (2001) *Cancer Res. 61*, 5692−5696.
7. Abraham, L., and Mackie, E. (1999) *J. Bone Miner. Res. 14*, 1320−1329.
8. Macfarlane, S., Seatter, M., Kanke, T., Hunter, G., and Plevin, R. (2001) *Pharm. Rev. 53*, 245−282.
9. O'Brien, P., Molino, M., Kahn, M., and Brass, L. (2001) *Oncogene 20*, 1570−1581.
10. Sambrano, G., Weiss, E., Zheng, Y., Huang, W., and Coughlin, S. (2001) *Nature 413*, 74−78.
11. Whitehead, I. P., Zohn, I. E., and Der, C. J. (2001) *Oncogene 20*, 1547−1555.
12. Reid, T., Bathoorn, A., Ahmadian, M. R., and Collard, J. G. (1999) *J. Biol. Chem. 274*, 33587−33593.
13. Reid, T., Furuyashiki, T., Ishizaki, T., Watanabe, G., Watanabe, N., Fujisawa, K., Morii, N., Madaule, P., and Narumiya, S. (1996) *J. Biol. Chem. 271*, 13556−13560.
14. Yoshida, E., Verrusio, E., Mihara, H., Oh, D., and Kwaan, H. (1994) *Cancer Res. 54*, 3300−3304.
15. Ren, X. D., and Schwartz, M. A. (2000) *Methods Enzymol. 325*, 264−272.
16. Kamath, L., Meydani, A., Foss, F., and Kuliopulos, A. (2001) *Cancer Res. 61*, 5933−5940.
17. Markwardt, F. (1986) *Ann. N.Y. Acad. Sci. 485*, 204−214.
18. Singer, S. J. (1967) *Adv. Protein Chem. 22*, 1−54.
19. Bodie, S. L., Ford, I., Greaves, M., and Nixon, G. F. (2001) *Biochem. Biophys. Res. Commun. 14*, 71−76.
20. Nishioka, H., Horiuchi, H., Tabuchi, A., Yoshioka, A., Shirakawa, R., and Kita T. (2001) *Biochem. Biophys. Res. Commun. 280*, 970−975.
21. Xu, W. F., Andersen, H., Whitmore, T. E., Presnell, S. R., Yee, D. P., Ching, A., Gilbert, T., Davie, E. W., and Foster, D. C. (1998) *Proc. Natl. Acad. Sci. U.S.A. 95*, 6642−6646.
22. Andersen, H., Greenberg, D., Fujikawa, K., Xu, W., Chung, D., and Davie, E. (1999) *Proc. Natl. Acad. Sci. U.S.A. 96*, 11189−11193.
23. Bauer, M., Retzer, M., Wilde, J. I., Maschberger, P., Essler, M., Aepfelbacher, M., Watson, S. P., and Siess, W. (1999) *Blood 94*, 1665−1672.
24. Kimura, K., Ito, M., Amano, M., Chihara, K., Fukata, Y., Nakafuku, M., Yamamori, B., Feng, J., Nakano, T., Okawa, K., Iwamatsu, A., and Kaibuchi, K. (1996) *Science 273*, 245−248.
25. Somlyo, A., Bradshaw, D., Ramos, S., Murphy, C., Myers, C., and Somlyo, A. (2000) *Biochem. Biophys. Res. Commun. 269*, 652−650.
26. Donovan, F. M., Pike, C. J., Cotman, C. W., and Cunningham, D. D. (1997) *J. Neurosci. 17*, 5316−5326.
27. Majumdar, M., Seasholtz, T. M., Goldstein, D., de Lanerolle, P., and Brown, J. H. (1998) *J. Biol. Chem. 273*, 10099−10106.
28. Seasholtz, T. M., Majumdar, M., Kaplan, D. D., and Brown, J. H. (1999) *Circ. Res. 84*, 1186−1193.
29. Carbajal, J. M., Gratrix, M. L., Yu, C. H., and Schaeffer, R. C., Jr. (2000) *Am. J. Physiol. Cell Physiol. 279*, C195−C204.
30. Evan-Ram, S., Uziely, B., Cohen, P., Grisaru-Granovsky, S., Maoz, M., Ginzburg, Y., Reich, R., Vlodavsky, I., and Bar-Shavit, R. (1998) *Nat. Med. 4*, 909−914.
31. Nystedt, S., Emilsson, K., Wahlestedt, C., and Sundelin, J. (1994) *Proc. Natl. Acad. Sci. U.S.A. 91*, 9208−9212.
32. Derian, C. K., Eckardt, A. J., and Andrade-Gordon, P. (1997) *Cell Growth Differ. 8*, 743−749.
33. Rubino, D., Driggers, P., Arbit, D., Kemp, L., Miller, B., Coso, O., Pagliai, K., Gray, K., Gutkind, S., and Segars, J. (1998) *Oncogene 16*, 2513−2526.
34. Toksoz, D., and Williams, D. A. (1994) *Oncogene 9*, 621−628.
35. Erickson, J. W., and Cerione, R. A. (2001) *Curr. Opin. Cell Biol. 13*, 153−157.
36. Ridley, A. (1999) in *Progress in Molecular and Subcellular Biology* (Jeauteur, J., Ed.) pp 1−16, Springer-Verlag, Heidelberg.
37. Tolias, K., Hartwig, J., Ishihara, H., Shibasaki, Y., Cantley, L., and Carpenter, C. (2001) *Curr. Biol. 10*, 153−156.
38. Vadlamudi, R., Li, F., Adam, L., Nguyen, D., Ohta, Y., Stossel, T., and Kumar, R. (2002) *Nat. Cell Biol. 4*, 681−690.

BI027100X